



Contents lists available at ScienceDirect

Infection, Genetics and Evolution

journal homepage: www.elsevier.com/locate/meegid



The association between the geographic distribution of *Triatoma pseudomaculata* and *Triatoma wygodzinskyi* (Hemiptera: Reduviidae) with environmental variables recorded by remote sensors

A.L. Carbajal de la Fuente^{a,*}, X. Porcasi^b, F. Noireau^{c,d}, L. Diotaiuti^e, D.E. Gorla^b

^a Depto. Entomologia, Instituto Oswaldo Cruz, FIOCRUZ, Pav. Carlos Chagas, Av. Brasil 4365, Manguinhos, Rio de Janeiro, Brazil

^b Centro Regional de Investigaciones Científicas y Transferencia Tecnológica, CRILAR, Entre Ríos y Mendoza s/n, (5301) Anillaco (La Rioja), Argentina

^c Institut de Recherche pour le Développement (IRD), UR016, Montpellier, France

^d IIBISMED, Facultad de Medicina, UMSS, Cochabamba, Bolivia

^e Instituto René Rachou, FIOCRUZ, Belo Horizonte, Brazil

ARTICLE INFO

Article history:

Received 27 March 2008

Received in revised form 27 September 2008

Accepted 30 September 2008

Available online xxx

Keywords:

Triatoma pseudomaculata

Triatoma wygodzinskyi

Geographic distribution

Environmental variables

Remote sensing

GIS

Chagas disease

ABSTRACT

In this study, predictive models of geographic distribution patterns of *Triatoma pseudomaculata* (Tps) and *T. wygodzinskyi* (Twy) were carried out. They were based on biophysical variables estimated from information provided by the satellite remote sensors AVHRR (Advanced Very High Resolution Radiometer) and MODIS (MODerate-resolution Imaging Spectroradiometer). Our goal was to analyze the potential geographic distribution of Tps and Twy and to assess the performance of three predictive models (one for each species and one for both species together) based on temperature, vapour pressure deficit, vegetation and altitude. The geographic distribution analysis shows that all models performed well (>85.7% of overall correct classification of presence and absence point data). The MODIS-based models showed lower correct classifications than the AVHRR-based models. The results strongly suggest that environmental information provided by remote sensors can be successfully used in studies on the geographic distribution of poorly understood Chagas disease vector species.

© 2008 Elsevier B.V. All rights reserved.

1. Introduction

The control of Chagas disease by elimination of domestic populations of *Triatoma infestans* (Klug, 1834) is being successfully pursued in most of the Southern Cone countries of South America, where this species was considered the main vector (Schofield et al., 2006). After Uruguay (1997) and Chile (1999), Brazil is the third country to obtain (2006) certification from the PAHO/WHO (www.paho.org/Spanish/DD/PIN/ps060616.htm) for having interrupted the transmission by *T. infestans*.

Triatoma pseudomaculata (Corrêa & Espínola, 1964) is the second most epidemiologically important species after *Triatoma brasiliensis* (Neiva, 1911) in the northeast of Brazil. Specimens typically inhabit sylvatic and peridomestic environments, but they occasionally enter human dwellings (Souza et al., 1999; Assis et al., 2007). *T. pseudomaculata* is considered an endemic species of the Caatinga and Cerrado biogeographic provinces (following the

biogeographic division proposed by Morrone, 2006) and has been recorded in the states of Alagoas, Bahia, Brasília, Ceará, Goiás, Maranhão, Mato Grosso do Sul, Minas Gerais, Paraíba, Pernambuco, Piauí, Rio Grande do Norte, Sergipe, and Tocantins (Carcavallo and Martínez, 1985; Carcavallo et al., 1998).

Despite the traditional view of *T. pseudomaculata* and *T. maculata* (Erichson, 1848) being closely related (*T. maculata* species complex *sensu* Carcavallo et al., 1998), recent studies have demonstrated a closer relationship between *T. pseudomaculata* and other Brazilian triatomines (Santos et al., 2007; Carbajal de la Fuente et al., 2008). One of these species, *T. wygodzinskyi* (Lent, 1951), is distributed in the south of Minas Gerais (Lent, 1951; Carcavallo et al., 1998) and São Paulo States (Carbajal de la Fuente et al., 2008). *T. wygodzinskyi* does not represent an epidemiological risk because it is restricted to the sylvatic environment. Both species share strong similarities in their external morphology (Lent and Wygodzinsky, 1979). Despite these morphological similarities and the close evolutionary relationship between *T. wygodzinskyi* and *T. pseudomaculata*, their ecological characteristics are markedly different. For example, in sylvatic environments, *T. wygodzinskyi* is rupicolous (Lent and Martins, 1940; Corrêa et al., 1965; Forattini et al., 1968, 1972; Barretto and Ribeiro,

* Corresponding author. Tel.: +55 21 2598 4320/22x117; fax: +55 21 2573 4468.
E-mail address: carbajal@ioc.fiocruz.br (A.L. Carbajal de la Fuente).

1981) while *T. pseudomaculata* is arboricolous (Dias-Lima et al., 2003; Noireau et al., 2005).

The biology, morphology, genetics and ecology of these species are increasingly being studied (Carbajal de la Fuente et al., 2007, 2008; Santos et al., 2007). Nevertheless, their geographic distribution is poorly understood, especially in the case of *T. wygodzinskyi*, which has only been recorded from the type locality (Lent, 1951; Lent and Wygodzinsky, 1979). The latest compilation of the geographic distribution of both species was presented by Carcavallo et al. (1998), and this paper is the first attempt to produce a predictive study of their distributions.

Satellite-based remote sensing offers significant benefits for many applications because it provides historical data for comparison and analysis (Ostfeld et al., 2005). One important application is in medical entomology where environmental variables obtained by remote sensors were used to elaborate the predictive models of the geographic distribution of several disease vectors (p. ex. Kitron et al., 1992, 1997; Kitron, 2000; Cromley and McLafferty, 2002; Getis et al., 2003; Snow et al., 2005; Kitron et al., 2006). This tool has been applied to study Chagas disease vectors in a few instances, mainly in studies of different species of *Triatoma*. Gorla (2001, 2002a, b) performed an analysis of the geographic distribution of some vectors such as *T. infestans*, *T. brasiliensis* and *Rhodnius pallescens* Barber, 1932. Costa et al. (2002) used the ecological niche modelling approach to characterize the ecological differentiation of *T. brasiliensis* populations in North-Eastern Brazil, and Peterson et al. (2002) used the same model to identify host relationships and predict the geographic distribution of *Triatoma protracta* complex, the species implicated in the transmission of Chagas disease in Mexico (see also Peterson, 2006). Dumonteil and Gourbière (2004) produced predictive models of *Triatoma dimidiata* (Latreille, 1811) distribution and elaborated risk maps for Chagas disease for the Yucatán peninsula (México). On the other hand, López-Cárdenas et al. (2005) modelled the ecological niches for five Mexican species of triatomine in Guanajuato State. Cecere et al. (2004) studied the spatio-temporal reinfestation patterns of *T. infestans* in a rural community of Argentina using a geographic information system, satellite imagery, and spatial statistics. Porcasi et al. (2006) analyzed the infestation of rural houses by *T. infestans* in the southern area of Gran Chaco in Argentina. Remotely sensed imagery can be used to carry out a fine temporal quantification of several environmental variables for particular geographic areas to obtain a precise characterization of species occurrence sites. This knowledge can be used to make predictions about the potential areas where the species might be present.

The goal of the present paper was to analyze the potential geographic distribution of *T. pseudomaculata* and *T. wygodzinskyi* through predictive models built from information derived from AVHRR (Advanced Very High Resolution Radiometer) and MODIS (MODerate-resolution Imaging Spectroradiometer) imagery. The geographic distribution models were compared to each other and contrasted with the currently known distribution of each species to select the best predictive model.

2. Material and methods

2.1. Geographic region of study

The data analysis was carried out within an area defined by the limits 0°N–30°S latitude and 30°W–60°W longitude. Field collections were conducted in the Brazilian states of Bahia, Ceará, Minas Gerais, Paraíba, São Paulo and Tocantins, geo-located using a handheld Garmin™ Legend GPS navigator (Fig. 1). The species occurrence dataset was constructed by the aggregation of published reports (1 site for *T. wygodzinskyi*) and field collections during the

present study (61 sites for *T. wygodzinskyi* and 168 for *T. pseudomaculata*). The environmental profile derived for the absence data was obtained from a random selection of points distributed in the biogeographic provinces of the Chaco-Caatinga-Cerrado corridor (Cabrera and Willink, 1973), excluding the distributional area proposed for the species by Carcavallo et al. (1998). A random selection of points for the species absence was performed for each one of three models: Twy, Tps (individual prediction for the distribution of *T. wygodzinskyi* and *T. pseudomaculata*, respectively) and Tps–Twy (both species combined in the same predictive model).

2.2. Environmental variables

The environmental variables used to characterize the presence and absence sites were estimated from two different types of satellite images, one produced by the AVHRR onboard the NOAA (National Oceanic and Atmospheric Administration) satellite series, and the other one produced by the MODIS onboard the TERRA (EOS AM 1- Earth Observing System-) satellite. For the analysis based on the AVHRR imagery, six environmental variables were used: air temperature (AT), land surface temperature (LST), mid-infrared radiation (MIR), normalized difference vegetation index (NDVI), vapour pressure deficit (VP), and digital elevation model (DEM). The first five variables were derived from a temporal series of monthly images taken from 1982 to 2000. The images had 8 km × 8 km spatial resolution. The temporal series was analyzed using Fourier temporal decomposition (image products were processed by the TALA Research Group, Oxford University) (Hay et al., 2006). The decomposition produced a set of 11 descriptive statistics for each variable: average (A0), minimum (Mn), maximum (Mx), amplitudes and phases of the annual, bi-annual and tri-annual cycles (A1, A2, A3, P1, P2, P3), the percentage of the total variance of the three first Fourier components (DALL), and the variance of the complete series (Vr). The AVHRR imagery plus the digital elevation model (DEM) constituted a set of 56 independent environmental properties for each pixel location (11 statistics for five environmental variables + DEM).

For the analysis based on the MODIS imagery, two environmental variables were used: land surface temperature (LST) and digital elevation model (DEM). The first variable was derived from a temporal series of weekly maximum values composite of diurnal (D) and nocturnal (N) images, taken between January 2003 and December 2004. The images had 1 km × 1 km spatial resolution. Eight descriptive statistics were produced for each variable: average (A0D, A0N, day and night respectively), minimum (MnD, MnN), maximum (MxD, MxN) and variance (VrD, VrN). The MODIS images were obtained from the EOS Data Gateway (<http://edcimswww.cr.usgs.gov/pub/imswelcome/>). These images are stored by the US Geological Service (USGS) in the Goode-Homolosine geographic projection. To standardize the geographic projection of the geospatial data in this study, the MODIS imagery were re-projected to the Latitude/Longitude Geographic Projection System using the projection tools of Idrisi Kilimanjaro v.14.02.

The land elevation was obtained from the digital elevation model (DEM) of the US Geological Service (USGS), with 90 m of spatial resolution. The DEM resolution was adjusted to 1 or 8 km depending on whether MODIS or AVHRR imagery was used, respectively. All image processing was carried out using Idrisi Kilimanjaro v.14.02.

2.3. Data analysis

Three models of geographic distribution were elaborated for each image type (AVHRR and MODIS): one model for *T.*



Fig. 1. Map showing the situation of the collecting localities: 1 = Sobral, CE; 2 = Bom Jesús, PB; 3 = Curaçá, BA; 4 = Itaberaba, BA; 5 = Senhor do Bom Fim, BA; 6 = Peixe, TO; 7 = Itaobim, MG; 8 = Santa Rita de Caldas, MG; 9 = Vargem Grande do Sul, SP; 10 = Ituparanga, SP; CE = Ceará State; PB = Paraíba State; BA = Bahia State; MG = Minas Gerais State; SP = São Paulo State.

wygodzinskyi (Twy), one for *T. pseudomaculata* (Tps) and one for the two species together (Twy–Tps). All the descriptive statistics for each environmental variable were used in the models. For each model, a stepwise discriminant analysis was performed in order to estimate the best set of variables that allowed the construction of a predictive model to recognize areas with similar environmental characteristics to the places of presence and absence of each species. The discriminant analysis was performed with STATISTICA v.7.0 (StatSoft, Inc. 2000). As the sample size did not allow the building of two independent subsamples for training sites and validation tests, the estimation of the misclassification rate was carried out using a cross-checked classification routine that iteratively build the discriminant equations leaving one data point out of the analysis for each iteration before calculating the classification matrix (PAD module developed by Dujardin, 2008).

3. Results

3.1. *T. wygodzinskyi* model (Twy)

3.1.1. AVHRR images

The discriminant analysis selected nine variables (A0, P1, P3, Vr of AT; A0, A1, Vr of VP; MIRMn and DEM) that classified correctly 100% of all absence sites (1023/1023 points) and 100% of the eight presence sites for *T. wygodzinskyi* (Wilks'-Lambda: 0.8579; $F(9, 907) = 16.68$, $p < 0.0001$). The classification functions and the

importance rank of the variables based on the standardized coefficients (taken as indicators of the relative weight) are shown in Table 1. The average (AT-A0) and variance (AT-Vr) of the air temperature and the annual amplitude of the vapour pressure deficit (VP-A1) were the variables with the highest contribution to the discrimination between the presence and absence sites. The predicted distribution of *T. wygodzinskyi* derived from AVHRR imagery is shown in Fig. 2a. The AVHRR imagery predicts a more extensive geographic distribution for *T. wygodzinskyi* than has been previously recorded. The predicted presence is not restricted only to the Minas Gerais State, but it is also predicted for the States of São Paulo, Rio de Janeiro, Paraná, Santa Catarina and Rio Grande do Sul.

3.1.2. MODIS images

The discriminant analysis selected three variables (DEM, LST-A0D and MnD) as the best for describing the geographic distribution of *T. wygodzinskyi*. These three variables classified correctly 91.1% of all absence sites (679/745 sites) and 90.9% of the presence sites (10/11 sites) (Wilks'-Lambda: 0.8905; $F(3, 752) = 30.81$, $p < 0.0001$). The classification functions and the importance rank of the variables based on the standardized coefficients are shown in Table 2. The land elevation (DEM) showed the highest weight in the analysis, followed by the average and the minimum of the diurnal land surface temperature (LST-A0D, MnD). The predicted distribution of *T. wygodzinskyi* derived from MODIS

Table 1
Standardized coefficients of the discriminant functions and coefficients of the presence/absences classifications sites for each AVHRR model (Tps = *Triatoma pseudomaculata*, Twy = *T. wygodzinskyi*).

Variable	Statistic	Twy model			Tps model			Twy–Tps model			
		SC	Absence function	Presence function	SC	Absence function	Presence function	SC	Absence function	Presence function (Twy)	Presence function (Tps)
AT	A0	–2.4406***	104.3087	103.8041	–0.2525	–0.8616	–0.8917	–0.5373*	73.3616	73.0576	73.2016
	P1	0.4215	–0.6096	–0.5608	–	–	–	–0.3286	–3.6850	–3.6395	–3.7197
	P3	0.3255	6.5542	6.6856	–	–	–	–	–	–	–
	Vr	–1.5905**	112.5461	112.0063	–	–	–	–	–	–	–
VP	A0	0.8257	–2.2852	–2.2798	–	–	–	0.3243	–1.5097	–1.5054	–1.5068
	A1	0.9072*	0.0758	0.0838	–	–	–	–	–	–	–
	A2	–	–	–	0.4256	–0.6551	–0.6364	0.4013	–0.5383	–0.5324	–0.5201
	Vr	0.8603	–7.6011	–7.5734	–	–	–	–	–	–	–
NDVI	A1	–	–	–	–0.6202	–2.8667	–2.9795	–	–	–	–
	A2	–	–	–	–1.0380**	1.7393	1.4084	–0.7934**	–6.6539	–6.6243	–6.8982
	A3	–	–	–	–	–	–	0.2821	3.7671	3.6670	3.9350
	P1	–	–	–	–0.5176	0.6131	0.3842	–	–	–	–
	P3	–	–	–	0.3833	2.5140	2.7744	0.4109	3.7751	3.7714	4.0498
	Vr	–	–	–	1.0708***	0.1220	0.2312	0.4470	0.5868	0.5811	0.6321
LST	A0	–	–	–	–0.4229	8.1189	8.0375	–	–	–	–
	Mn	–	–	–	0.9476*	0.0833	0.2258	0.8982***	–19.7272	–19.6714	–19.5888
MIR	A2	–	–	–	0.4558	1.5685	2.1752	0.3086	37.8825	37.5940	38.2524
	P1	–	–	–	–	–	–	0.3437	9.9216	9.9054	10.0070
	Mn	0.4962	–5.7836	–5.7005	–	–	–	–	–	–	–
DEM		0.1876	2.2183	2.2216	–	–	–	–0.0026	0.7474	0.7575	0.7483
Constant		–	–148729.6719	–147473.1406	–	–12480.2002	–12671.9893	–	–80841.1719	–80107.1484	–80812.0703

SC = Standardized coefficients; AT = Air temperature; VP = Vapor pressure deficit; NDVI = Normalized difference vegetation index; LST = Land surface temperature; MIR = Mean of the infrared radiation; DEM = Land elevation. A0 = Average; A1, A2 and A3 = Amplitudes of the 1, 2, 3-annual cycles; P1, P3 = Phase of 1, 3-annual cycles; Vr = Variance; Mn = Minimum.

* Variables weight.

** $P < 0.01$.

*** $P < 0.01$.

imagery is shown in Fig. 2b. The model predicts a distribution throughout the States of Bahia, Minas Gerais, Espírito Santo, Rio de Janeiro, São Paulo, Paraná, Santa Catarina and Rio Grande do Sul.

3.2. *T. pseudomaculata* model (Tps)

3.2.1. AVHRR images

The discriminant analysis selected 10 variables (P1 of AT; A1, A2, P1, P3, Vr of NDVI; A2 of VP; A0, Mn of LST and A2 of MIR) that classified correctly 98.4% of all absence sites (438/445 points) and 76.2% of the presence sites (16/21 sites) (Wilks'-Lambda: 0.4825, $F(10, 455) = 48.78, p < 0.0001$). The classification functions and the importance rank of the variables based on the standardized coefficients are shown in Table 1. The total variance of the time series and the bi-annual amplitude of the normalized difference vegetation index (Vr and A2 of NDVI) together with the minimum land surface temperature (Mn of LST) were the variables that

discriminated the best between the presence and absence sites. The predicted distribution of *T. pseudomaculata* derived from AVHRR imagery is shown in Fig. 2c. This model shows a predicted geographic distribution throughout the states of Alagoas, Bahia, Brasília, Ceará, Goiás, Maranhão, Mato Grosso do Sul, Minas Gerais, Paraíba, Pernambuco, Piauí, Rio Grande do Norte, Sergipe and Tocantins.

3.2.2. MODIS images

The discriminant analysis identified three variables (DEM, LST-AOD and MxN) with the ability to classify correctly 97.2% of all absence sites (376/387 sites) and 78.4% of the presence sites (30/38 sites) (Wilks'-Lambda: 0.5805; $F(3, 421) = 101.39, p < 0.0001$). The classification functions and the importance rank of the variables based on the standardized coefficients are shown in Table 2. The maximum of the nocturnal land surface temperature (LST-MxN) showed the highest weight, followed by the land elevation (DEM) and the average of the diurnal land surface

Table 2
Standardized coefficients of the discriminant functions and coefficients of the presence/absence classifications sites for each MODIS model (Tps = *Triatoma pseudomaculata*, Twy = *T. wygodzinskyi*).

Variable	Statistic	Twy model			Tps model			Twy–Tps model			
		SC	Absence function	Presence function	SC	Absence function	Presence function	SC	Absence function	Presence function (Twy)	Presence function (Tps)
LST	AOD	–0.3615	3.5680	3.1995	–0.4992	34.052	4.004	–0.5178	3.4383	3.0000	4.0400
	MnD	–0.2009	0.2315	0.0948	–	–	–	–	–	–	–
	MxN	–	–	–	–1.0415	8.8724	10.3094	–1.0136	8.9740	9.3816	10.4289
DEM		0.8541	0.0095	0.0193	–0.7807	0.0641	0.0735	–0.7008	0.0647	0.0785	0.0743
Constant		–	–58.2271	–56.6870	–	–160.8798	–220.6814	–	–162.6489	–223.0338	–172.7599

SC = Standardized coefficients; AOD = Diurnal average; MnD = Minimum diurnal; MxN = Maximum nocturnal; DEM = Land elevation.

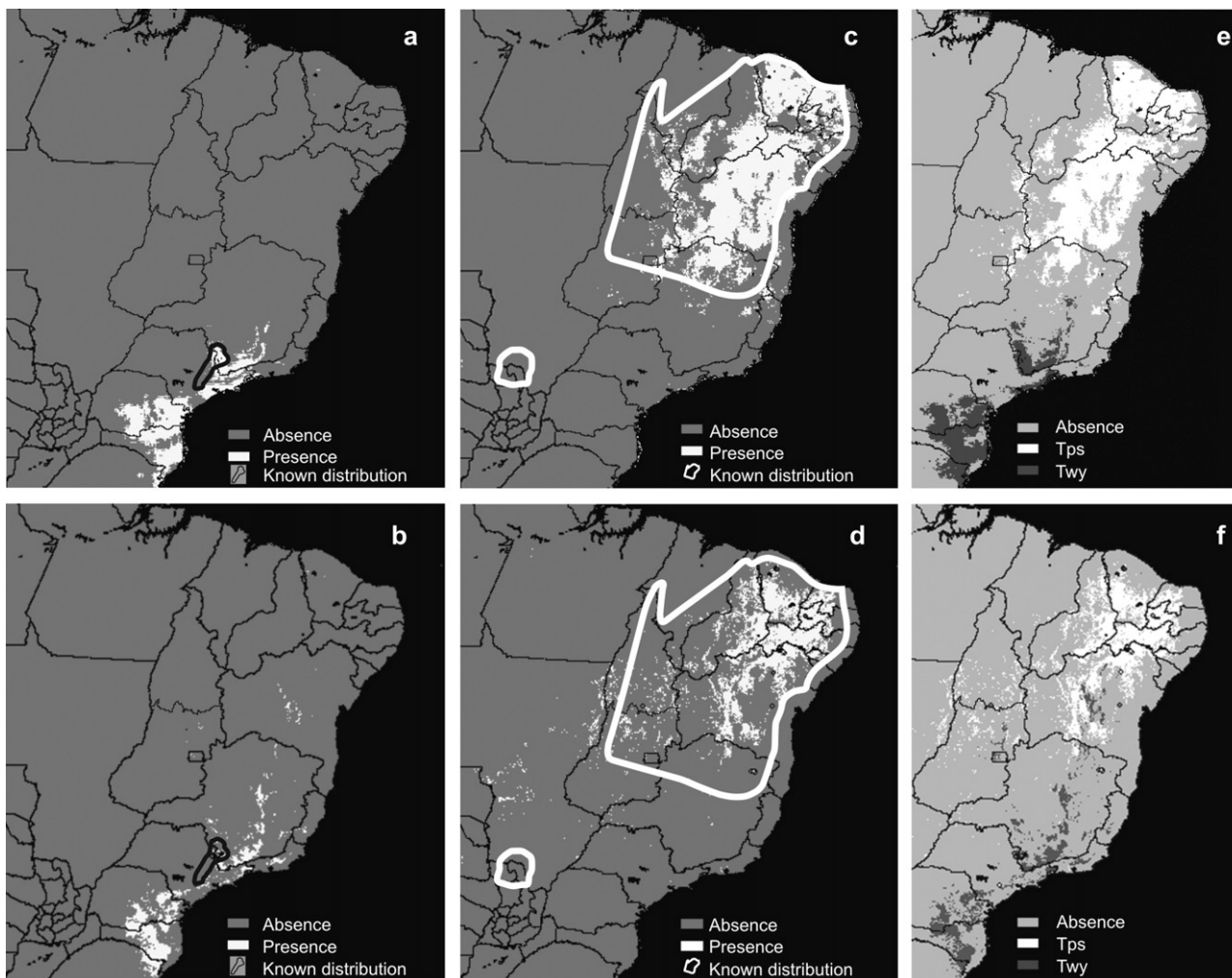


Fig. 2. Presence and absence areas of *T. wygodzinskyi* and *T. pseudomaculata* for each three models proposed: Twy (a and b), Tps (c and d) and Twy–Tps (e and f). The areas were predicted analyzing AVHRR (a, c, and e) and MODIS (b, d, and f) images. The known distribution of *T. wygodzinskyi* (after Carcavallo et al., 1998 and Forattini et al., 1972) is represented by a black polygon (a and b). The known distribution of *T. pseudomaculata* (after Carcavallo et al., 1998) is represented by a white polygon (a and b).

temperature (LST-AOD). The predicted distribution of *T. pseudomaculata* derived from MODIS imagery is shown in Fig. 2d. In this model, the presence of this species is expanded to the Espírito Santo State but excludes the Mato Grosso do Sul State.

3.3. *T. wygodzinskyi*–*T. pseudomaculata* model (Twy–Tps)

3.3.1. AVHRR images

The discriminant analysis selected 12 variables (A0 and P1 of AT; A2, A3, P3 and Vr of NDVI; A2 and P1 of MIR; A0 and A2 of VP; Mn of LST and DEM) to classify correctly 94.6% of all absence sites (469/496 points), 87.5% of the *T. wygodzinskyi* presence sites (7/8 sites) and 80.9% of the *T. pseudomaculata* presence sites (17/21 sites) (Willks-Lambda: 0.4243; $F(24, 1022) = 22.78, p < 0.0001$). The classification functions and the importance rank of the variables based on the standardized coefficients are shown in Table 1. The average air temperature (AT-A0) and the bi-annual amplitude of the normalized difference vegetation index (NDVI-A2) followed by the minimum land surface temperature (LST-Mn) were the variables with the highest contribution to the discrimination between the presence and absence sites. The predicted distribution observed in the conjunct model of both *T. wygodzinskyi* and *T. pseudomaculata* derived from AVHRR imagery is represented in Fig. 2e. The distribution of both species is similar to the

distribution predicted in the models for each single species exhibiting identical distributional pattern.

3.3.2. MODIS images

The discriminant analysis selected three variables (DEM, LST-AOD and MxN) that classify correctly 89.0% of all absence sites (341/383 sites), 90.9% of the *T. wygodzinskyi* presence sites (10/11 sites) and 78.9% of the *T. pseudomaculata* presence sites (30/38 sites) (Willks-Lambda: 0.4693; $F(6, 854) = 65.41, p < 0.0001$). The classification functions and the importance rank of the variables based on the standardized coefficients are shown in Table 2. The maximum nocturnal land surface temperature (LST-MxN) showed the highest contribution followed by the land elevation (DEM) and the average of the diurnal land surface temperature (LST-AOD). The predicted distribution observed in the *T. wygodzinskyi*–*T. pseudomaculata* model derived from MODIS imagery is represented in Fig. 2f. As observed in the joint model based on AVHRR imagery, the distribution of both species is similar to the distribution predicted in the single models for each species.

4. Discussion

The present work compares for the first time predictive models derived from AVHRR and MODIS imagery, in order to identify the

potential geographic range of two Chagas disease vector species. The comparative analysis between the AVHRR and MODIS imagery showed that they had different abilities to correctly classify the species' presence/absence sites. The best models were obtained using AVHRR data and showed correct classification of presence/absence sites more than 94% of the time. In each case from the MODIS imagery, fewer presence sites were correctly classified than those from the corresponding AVHRR imagery. The worse predictive model used MODIS imagery for *T. wygodzinskyi* and showed only 88.2% correct classifications. This lower performance could be attributed to the fact that the models based on MODIS images did not include the AT and VP variables (only LST and DEM), precisely the variables with the highest discrimination power for the presence sites in the AVHRR Twy model. The predictive map derived from the AVHRR and MODIS images for the two species case (Twy–Tps model), showed very similar equivalent distributional areas for both species. The most conspicuous difference was the reduction of the distribution area for *T. pseudomaculata* in the MODIS Twy–Tps prediction map (Fig. 2f).

Compared with the AVHRR data, the higher 1 km × 1 km resolution of the MODIS imagery increased the number of presence site data for both species (8–11 for *T. wygodzinskyi* and 21–38 for *T. pseudomaculata*), but this increment did not significantly affect model performance. Contrary to expected, the models based on the coarser grained scale data (AVHRR imagery) showed higher predictive efficiency than the models obtained from the fine-grained scale data (MODIS imagery). This could be related to the

higher number of environmental variables considered in the AVHRR imagery (56 variables) compared to the lower number in the MODIS set (9 variables), as opposed to a result of the different spatial resolution of each kind of image. Also, the temporal AVHRR series (1982/2000) is longer than the temporal MODIS series (2003/2004).

The Twy model derived from AVHRR images classified correctly 100% of the presence and absence sites and was the best predictive model. Five of the nine variables in the discriminant model are elevation and temperature indicators along the “Serra da Mantiqueira” range, spanning 1000 m of altitude. The Tps model derived from AVHRR images shows a predicted geographic distribution coincident with the distribution areas proposed by Carcavallo et al. (1998). The Tps model predicts the existence of *T. pseudomaculata* in the States of Alagoas, Bahía, Brasília, Ceará, Goiás, Espírito Santo, Minas Gerais, Paraíba, Pernambuco, Piauí, Rio Grande do Norte, Maranhão and Sergipe. Comparing the predicted distribution with the distribution proposed by Carcavallo et al. (1998), the model expands the presence of this species to the Espírito Santo State but excludes the State of Mato Grosso do Sul. It is a good predictive model, correctly classifying 76.2 % of the presence and 98.4% of absence sites.

For *T. pseudomaculata*, the variables with the highest discriminant power between the presence and absence sites are related to the vegetation (NDVI) and the land surface temperature (LST). These variables were not included in the Twy model. The total number of discriminant variables for each model (9 for Twy,

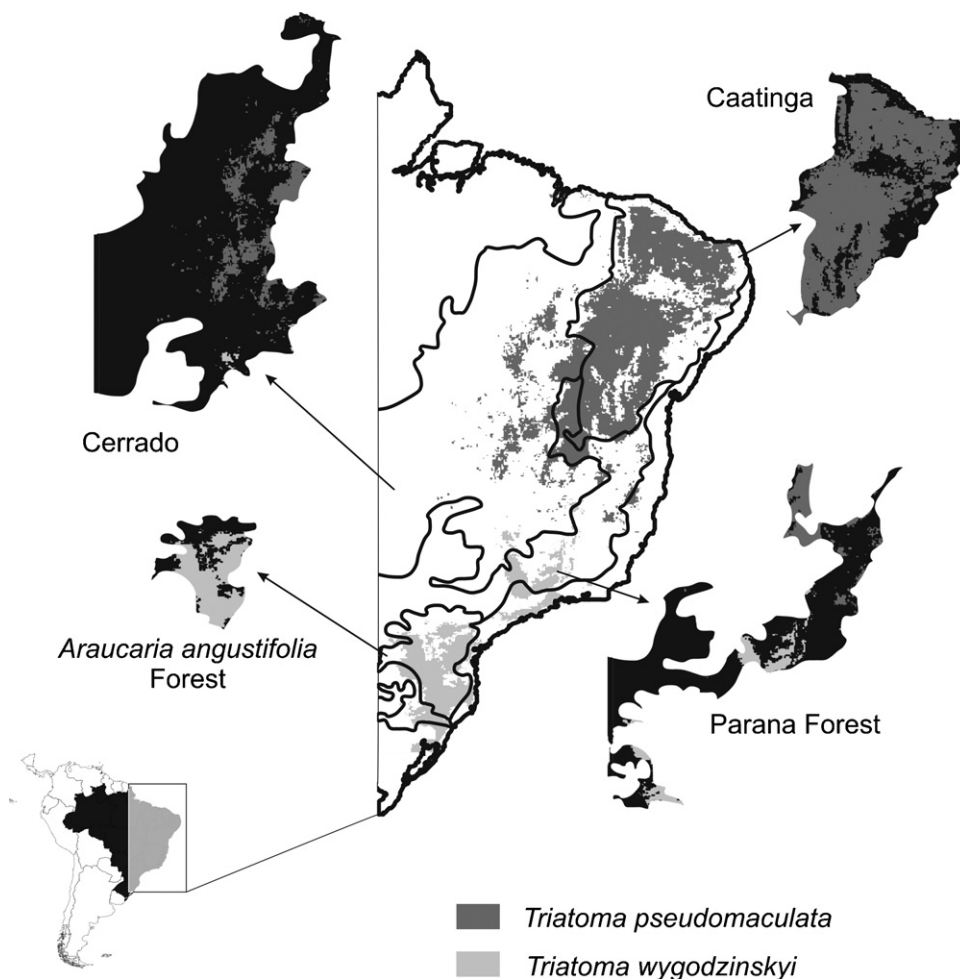


Fig. 3. Predicted distribution of *T. wygodzinskyi* and *T. pseudomaculata* (AVHRR images, Twy–Tps model) in the context of Morrone (2006) biogeographic provinces: Caatinga, Cerrado, Paraná forest and *Araucaria angustifolia* forest.

10 for Tps and 12 for Twy–Tps) is high compared to similar studies of *T. infestans* (Gorla, 2002b), *R. pallenscens*, *R. colombiensis* and *R. ecuadoriensis* (Gorla et al., 2005), where six and seven variables were needed, respectively, for geographic distribution models that classified correctly >90% of the data points. This greater number of environmental variables suggests that the geographic distribution of *T. pseudomaculata* is not associated with the studied environmental variables as strongly as the distribution of *T. wygodzinskyi*. The models obtained do not show an evident sympatric area for the studied species. The absence of a sympatric area and the identification of a different environmental variable set to describe the geographic distribution suggest that the occurrence of these two species is defined by different environmental features at the regional scale. An interesting parallel can be made with the biogeographic provinces of South America proposed by Morrone (2006), using panbiogeographic and cladistic analyses of the entomofauna. Within this biogeographic context, the predicted distribution of *T. pseudomaculata* in our study is mainly associated with Caatinga and areas of Cerrado (Fig. 3), the two main Brazilian xerophitic ecosystems. By contrast, the predicted distribution of *T. wygodzinskyi* is associated with the Paraná Forest and the *Araucaria angustifolia* Forest provinces (Fig. 3). The association between *T. wygodzinskyi* occurrence and the “forest” biogeographic provinces is not reflected by the inclusion of the vegetation index in the predicted distribution model, although this could be related to the rupicolous behaviour of the species. This microhabitat preference could be responsible for the species’ survival in areas where the original forest was strongly fragmented or even eliminated. Presence sites included localities with and without forest cover, and this is the probable reason of the low influence of the vegetation variables in the prediction of *T. wygodzinskyi* distribution. The situation is different for *T. pseudomaculata*. As the species is arboricolous in a sylvatic ecosystem, the vegetation cover will necessarily affect its distribution, as the absence of vegetation means species absence. This species is rupicolous in sylvatic habitat, and shows a strong association with the xerophitic environment of Caatinga and Cerrado. These two biogeographic areas have a unique vegetation conformation, and it is possible that the remotely sensed vegetation variables reflect the species’ spatial delimitation and can be considered good indicators for the distribution of the two species. Concerning the triatomine species, information about their suitability for a given habitat arises only from studies performed on a coarse-grained scale. Studies at other spatial scales must be undertaken.

The obtained distributional maps for *T. pseudomaculata* and *T. wygodzinskyi* were highly congruent with the pre-existing presence data of the two species and expand their range to potential new areas. Our results strongly suggest that the environmental information provided by remote sensors may be successfully used in predictive studies about the geographic distribution of Chagas disease vectors.

Acknowledgments

We are indebted to the anonymous referees for their help improving the manuscript. Special thanks to C.M. Lopes, P. Araújo, J.M.S. Barata, R. Hoffman, G.A. Grande, E. da Rocha, J.P. da Silva and C.M. Neves for their invaluable help and assistance with the fieldwork. Thanks to M. Lamfri, M. Scavuzzo and C. Rotela (Gulich Institute, CONAE, Argentina) for support during the MODIS imagery download, and to C.E. Almeida for providing the geographic coordinates of *T. pseudomaculata* in Paraíba State. Thanks to A. Pérez González for the suggestions on an early version of the manuscript. This study received financial support from the Network ECLAT-CDIA (European Community), IRD

(France) and FIOCRUZ (Brazil). A.L.C.F. has a grant from CAPES-EL Nacional, Brazil. X.P. and D.E.G. are members of “Consejo Nacional de Investigaciones Científicas y Tecnológicas” (CONICET), Argentina.

References

- Assis, G.F.M., Azeredo, B.V.M., Carbajal de la Fuente, A.L., Diotaiuti, L., Lana, M., 2007. Domiciliation of *Triatoma pseudomaculata* (Côrrea & Espínola, 1964) in the Jequitinhonha Valley, State of Minas Gerais Brazil. *Rev. Bras. Med. Trop.* 40, 391–396.
- Barretto, M.P., Ribeiro, R.D., 1981. Estudo sobre reservatórios e vetores silvestres do *Trypanosoma cruzi*. LXXVII. Observações sobre a ecologia do *Triatoma arthurmeivai* Lent & Martins, 1940 (Hemiptera, Reduviidae). *Rev. Bras. Biol.* 41, 317–320.
- Cabrera, A., Willink, A., 1973. Biogeografía de América Latina. Serie de Biología 13. OEA Press, Washington DC, pp. 1–120.
- Carbajal de la Fuente, A.L., Minoli, S.A., Lopes, C.M., Noireau, F., Lazzari, C., Lorenzo, M., 2007. Captures of flying *Triatoma brasiliensis* and *Triatoma pseudomaculata* (Hemiptera: Reduviidae) by means of battery-powered light traps. *Acta Tropica*. 101, 115–119.
- Carbajal de la Fuente, A.L., Noireau, F., Catalá, S., 2008. Inferences about antennal phenotype: the *Triatoma maculata* complex (Hemiptera: Triatominae) is valid? *Acta Tropica*. 106, 16–21.
- Carcavallo, R.U., Martínez, A., 1985. Biología, ecología y distribución geográfica de los triatomíneos americanos. In: Carcavallo, R.U., Rabinovich, J.E., Tonn, R.J. </ED> (Eds.), Factores biológicos y ecológicos en la enfermedad de Chagas. OPS-ECO/MSAS-SNCH, Buenos Aires, pp. 149–208.
- Carcavallo, R.U., Curto de Casas, S.I., Sherlock, I.A., Galíndez Girón, I., Jurberg, J., Galvão, C., Segura, C.A.M., Noireau, F., 1998. Geographical distribution and altitudinal dispersion. In: Carcavallo, R.U., Galíndez Girón, I., Jurberg, J., Lent, H. (Eds.), Atlas of Chagas Disease Vectors in the Americas. FIOCRUZ, Rio de Janeiro, Brazil, pp. 561–600.
- Cecere, M.C., Vazquez-Prokopec, G.M., Gürtler, R., Kitron, U., 2004. Spatio-Temporal Analysis of Reinfestation by *Triatoma infestans* (Hemiptera: Reduviidae) Following Insecticide Spraying in a Rural Community in Northwestern Argentina. *Am. J. Trop. Med. Hyg.* 71 (6), 803–810.
- Corrêa, R.R., Alves, U.P., Noda, J., 1965. Nota sobre o *Triatoma arthurmeivai*. Seu criadouro extradomiciliar (Hemiptera, Reduviidae). *Revista Brasileira de Malariologia e Doenças Tropicais* 17, 217–232.
- Costa, J., Peterson, A.T., Beard, C.B., 2002. Ecological niche modeling and differentiation of populations of *Triatoma brasiliensis* Neiva 1911 the most important Chagas disease vector in northeastern Brazil (Hemiptera, Reduviidae Triatominae). *Am. J. Trop. Med. Hyg.* 67, 516–520.
- Dias-Lima, A.G., Menezes, D., Sherlock, I., Noireau, F., 2003. Wild habitat and related fauna of *Panstrongylus lutzi* (Reduviidae Triatominae). *J. Med. Entomol.* 40, 989–990.
- Dujardin JP., 2008. PAD (Permutaciones y Análisis Discriminante). <http://www.mpl.ird.fr/morphometrics/pad/index.html>.
- Dumontel, E., Gourbière, S., 2004. Predicting *Triatoma dimidiata* abundance and infection rate: a risk map for natural transmission of Chagas disease in the Yucatán peninsula of Mexico. *Am. J. Trop. Med. Hyg.* 70 (5), 514–519.
- Cromley, E.K., McLafferty, S.L., 2002. GIS and Public Health. The Guilford Press.
- Forattini, O.P., Juarez, E., Rabello, E.X., 1968. Dados sobre a biologia do *Triatoma arthurmeivai* no sudeste do Estado de São Paulo, Brasil (Hemiptera Reduviidae). *Rev. Saude Publica* 2, 186–193.
- Forattini, O.P., Rabello, E.X., Pattoli, D.B., 1972. Aspectos ecológicos da tripanossomose Americana IV- Mobilidade de *Triatoma arthurmeivai* em seus ecótopos naturais. *Rev. Saude Publica* 6, 183–187.
- Getis, A., Morrison, A.C., Gray, K., Scott, T.W., 2003. Characteristics of the spatial pattern of the dengue vector, *Aedes aegypti*, in Iquitos Peru. *Am. J. Trop. Med. Hyg.* 6, 494–505.
- Gorla, D.E., 2001. Análisis de la distribución geográfica de Triatominae a escala continental en base a información de variables ambientales. *Unlar Ciencia* 2, 2–8.
- Gorla, D.E., 2002a. Variables ambientales registradas por sensores remotos como indicadores de la distribución geográfica de *Triatoma infestans* (Heteroptera: Reduviidae). *Ecología Austral* 12, 117–127.
- Gorla, D.E., 2002b. La reconstrucción de la distribución geográfica de Triatominae en base a información de variables ambientales. In: Proceedings of the Fourth International Workshop on Population Genetics and Control of Triatominae (ECLAT). Universidad de los Andes Press, Isla Barú, Colombia, CIMPAT, Colombia, pp. 167–173.
- Gorla, D.E., Porcasi, X., Catalá, S.S., 2005. Sistemas de información geográfica y sensores remotos como herramientas en los programas de control vectorial de la enfermedad de Chagas. In: Proceedings of the First International Workshop on Control of Chagas Disease. Universidad de los Andes Press, Bogotá, Colombia, pp. 265–278.
- Hay, S.I., Tatem, A.J., Graham, A.J., Goetz, S.J., Rogers, D.J., 2006. Global environmental data for mapping infectious disease distribution. *Adv. Parasitol.* 62, 38–79.
- Kitron, U., 2000. Risk maps: transmission and burden of vector-borne diseases. *Parasitol. Today* 16, 324–325.

- Kitron, U., Jones, C.J., Bouseman, J.K., Nelson, J.A., Baumgartner, D.L., 1992. Spatial analysis of the distribution of *Ixodes dammini* (Acari: Ixodidae) on white-tailed deer in Ogle county, Illinois. *J. Med. Entomol.* 29, 259–266.
- Kitron, U., Michael, J., Swanson, J., Haramis, L., 1997. Spatial analysis of the distribution of LaCrosse encephalitis in Illinois, using a geographic information system and local and global spatial statistics. *Am. J. Trop. Med. Hyg.* 57, 469–475.
- Kitron, U., Clennon, J.A., Cecere, M.C., Gürtler, R.E., King, C.H., Vazquez-Prokopec, G., 2006. Upscale or downscale: applications of fine scale remotely sensed data to Chagas disease in Argentina and schistosomiasis in Kenya. *Geospat. Health* 1, 49–58.
- Lent, H., 1951. Novo *Triatoma* no Estado de Minas Gerais (Brasil) (Hemiptera: Reduviidae). *Revista Entomologia* 22 (1-3), 349–353.
- Lent, H., Martins, A.V., 1940. Estudos sobre os triatomídeos de Minas Gerais, com descrição de uma espécie nova. *Revista de Entomologia* 11, 877–886.
- Lent, H., Wygodzinsky, P., 1979. Revision of the Triatominae (Hemiptera, Reduviidae), and their significance as vectors of Chagas disease. *Bull. Am. Museum Nat. Hist.* 163, 127–520.
- López-Cárdenas, J., Gonzalez Bravo, Schettino, F.E., Gallaga Solórzano, J.C., Ramírez Barba, E., Martínez Mendez, J., Sánchez-Cordero, V., Peterson, A.T., Ramsey, J.M., 2005. Fine-scale predictions of distributions of Chagas disease vectors in the state of Guanajuato, Mexico. *J. Med. Entomol.* 42 (6), 1068–1081.
- Morrone, J., 2006. Biogeographic areas and transition zones of Latin America and the Caribbean islands based on panbiogeographic and cladistic analyses of the entomofauna. *Annu. Rev. Entomol.* 51, 467–494.
- Noireau, F., Carbajal de la Fuente, A.L., Lopes, C.M., Diotaiuti, L., 2005. Some considerations about the ecology of Triatominae. *An. Acad. Bras. Cien.* 77, 1–6.
- Ostfeld, R.S., Glass, G.E., Keesing, F., 2005. Spatial epidemiology: an emerging (or re-emerging) discipline. *Trends Ecol. Evol.* 20, 328–336.
- Peterson, A.T., 2006. Ecologic niche modeling and spatial patterns of disease transmission. *Emerg. Infect. Dis.* 12 (2), 1822–1826.
- Peterson, A.T., Sánchez-Cordero, V., Beard, C.B., Ramsey, J.M., 2002. Ecologic niche modeling and potential reservoirs for Chagas disease. *Mexico Emerg. Infect. Dis.* 8, 662–667.
- Porcasi, X., Catalá, S.S., Hrellac, H., Scavuzzo, M.C., Gorla, D.E., 2006. Infestation of rural houses by *Triatoma infestans* (Hemiptera: Reduviidae) in southern area of Gran Chaco in Argentina. *J. Med. Entomol.* 43 (5), 1060–1067.
- Santos, S.M., Lopes, C.M., Dujardin, J.P., Panzera, F., Perez, R., Carbajal de la Fuente, A.L., Pacheco, R., Noireau, F., 2007. Evolutionary relationships based on genetic and phenetic characters between *Triatoma maculata* *Triatoma pseudomaculata* and morphologically related species (Reduviidae: Triatominae). *Infect. Genet. Evol.* 7, 469–475.
- Schofield, C., Jannin, J., Salvatella, J.R., 2006. The future of Chagas disease control. *Trends Parasitol.* 22 (12), 583–588.
- Souza, L.C., Frota, F.C.C., Souza, J.A., Lima, J.W.O., 1999. Descrição de um foco urbano de *Triatoma pseudomaculata* (Hemiptera: Reduviidae: Triatominae), na cidade de Sobral, norte do Ceará Resultados preliminares. *Rev. Soc. Bras. Med. Trop.* 32, 84–85.
- Snow, R.W., Guerra, C.A., Noor, A.M., Myint, H.Y., Hay, S.I., 2005. The global distribution of clinical episodes of *Plasmodium falciparum* malaria. *Nature* 434, 214–217.